Mechanical Spectroscopy and Internal Friction in SiO₂/Si

A.P. Onanko[1], V.V. Kuryliuk[1], Y.A. Onanko[2], A.M. Kuryliuk[1], D.V. Charnyi[2], O.P. Dmytrenko[1],
M.P. Kulish[1], T.M. Pinchuk-Rugal[1], A.A. Kuzmych[3]

[1] *Taras Shevchenko National University of Kyiv, 64/13, Volodymyrska St., 01601 Kyiv, Ukraine*
[2] *Institute of Water Problems and Land Reclamation, 37, Vasylkivska St., 03022 Kyiv, Ukraine*
[3] *National University of Water and Environmental Engineering, 11, Soborna St., 33000 Rivne, Ukraine*

The method was developed, the installation was designed and manufactured for excitation and registration of damped bending resonant oscillations in SiO₂/Si disc-shaped wafer-plates with thickness $h_S = 300 \div 500 \cdot 10^3$ nm and diameter $D = 60 \div 100 \cdot 10^{-3}$ m with the aim to measure structurally sensitive internal friction (IF) Q^{-1}. The technique for non-destructive testing of the integral density of structural defects n_d and the depth of the broken layer h_{bl} in disk-shaped semiconductor substrates was developed. The measurement of IF background $Q^{-1}{}_0$ at harmonic frequencies f_0, f_2 allowed to experimentally determine the nodal lines of oscillating disks. This allowed to make corrections to theoretical calculations of finding these nodal lines, taking into account the linear dimensions of the disks and the method of their attachment. Temperature IF spectrum $Q^{-1}(T)$ in SiO₂/Si disk-like wafer-plates after their X-ray and electron irradiation was studied. It was found that annealing of Si structural defects changes the shape of the temperature IF spectrum $Q^{-1}(T)$ in the measurements process. IF peaks $Q^{-1}{}_M$, which is formed by point defects, could be observed under the condition that a SiO₂/Si wafer-plate was heated with velocity $V = \Delta T / \Delta t \le 0.1$ K/c. This made it possible to determine the activation energy H of the reorientation of radiation defects anisotropic complexes. The establishment of the stability of IF background parameters $Q^{-1}{}_0$ made it possible to determine the radiation resistance of semiconductor wafer-plates and devices based on them. The proposed methodology can be used as a non-destructive method to control the crystal structure defects of semiconductor wafer-plates used for microelectronics.

Keywords: Mechanical spectroscopy, Relaxation mechanism, Substrate, Migration of atoms, Internal friction.

1. INTRODUCTION

The physical properties of semiconductor crystals significantly depend on the presence of crystal lattice defects. These defects primarily affect the electrical and optical properties of semiconductor crystals. Such characteristics of semiconductor devices as current I, breakdown voltage U_{BV}, noise I_N significantly depend on the defect current I_D, defect density n_d, defect mobility μ and the interaction between defects. Vacancies (V) in Si depending on the magnitude of the charge V^+ have different values of the migration energy E_M and annealing temperature T_{an} [1-4].

Parameters of semiconductor crystals essentially depend on their structural perfection. Since the main material of semiconductor substrates in various microelectronics products is Si, it is first necessary to study the dynamics of defects in the crystal structure of Si during irradiation. Among the methods of studying structural defects in these crystals the promising method is the structure-sensitive method of internal friction (IF), which makes it possible to study the dynamics of dislocations. The structure-sensitive method of IF mechanical relaxation was used to study the presence of structure defects, their dynamics. Mechanical relaxation of the elastic deformed semiconductor crystal is manifested as the elastic aftereffect, elastic hysteresis σ-ε, creep – deformation $\varepsilon(t)$ at constant stress σ_0, stress relaxation $\sigma(t)$ at constant deformation ε_0 [5-8].

The electrophysical properties of semiconductor devices significantly depend on the perfection of their structure. It is necessary to control the structure of semiconductor disk-shaped wafer-plates in the manufacture of large integrated circuits (LIC). The technique was developed, and the device was made allowing to obtain the information about structural defects in such disks by attenuating elastic oscillations Q^{-1} to study the defect density n_d and the depth h_d of their propagation. This technique takes into account the position of mechanical relaxation and that the amount of scattered energy of mechanical vibrations depends on the number of scattering centers. This is the IF dependence on the crystal structure defects. It is possible to study the dynamic behavior of defects by the IF method and the interaction of dislocations with point defects by the amplitude-dependent IF. The amplitude-independent IF provides information on the resistance force F of dislocations in the crystal lattice [9-11].

Vacancies V and interstitial atoms Si_i can combine into macroscopic defects up to $1000 \div 2000$ nm in size. Such incorporations can capture impurity atoms whose radii are significantly different from the radii of Si atoms. This process is energetically advantageous, since impurity atoms within the inclusion contribute to the reduction of the deformation potential U of the Si lattice near the inclusion. The formation of the V-V vacancy by combining two vacancies leads to the reduction of the broken ties number, which is energy efficient. The interaction of the vacancy V with the interstitial atom Si_i is also energetically beneficial, which leads to the annihilation of these defects. The formation of the vacancy complex V and the impurity atom $V + B$ also reduces the elastic energy E_{el} of the crystal lattice distortion, and therefore such a process is energetically advantageous [12-15].

2. MATERIALS AND METHODS

The study of structural defects in thin SiO_2/Si wafer-plates with $h \approx 400 \cdot 10^3$ nm thickness becomes topical with the development of microelectronics. IF method makes it possible to study defect formation during the formation of SiO_2/Si structures. The measurements were carried out at frequencies $f_1 \approx 653$ Hz, $f_2 \approx 1350$ Hz at low strains $\varepsilon \approx 10^{-6} \div 10^{-7}$, excluding plastic deformation, and at high temperatures T on the same sample during the entire technological cycle of obtaining SiO_2/Si structures.

The main characteristics of SiO_2/Si wafer-plates that determine their behavior under irradiation are.

1. Concentration and type of structural defects or impurity atoms, which capable of interacting with components of primary radiation defects (RD) – V-Si_i, forming electrically active secondary RD.

2. The concentration of electrically active defects or impurities that affect RD charge state, the efficiency of their interaction with each other and with other charged centers.

3. Concentration and type of impurity or structural defects-getters, which capable of interacting with primary RD without the formation of electrically active secondary RD.

The measurement of IF temperature dependences $Q^{-1}(T)$ was performed on p-type Si wafer-plates, orientation (100), boron-doped B, with specific electrical resistance $\rho \approx 7.5$ Ohm cm, thickness $h \approx 460 \cdot 10^3$ nm after application of SiO_2 layer with thickness $h_{SiO2} \approx 100$ nm in Fig. 1 as the result of high-temperature oxidation in dry O_2 at $T_0 \approx 1300$ K.
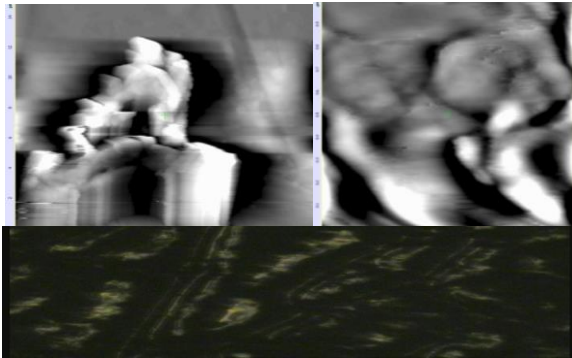

Fig. 1 – 3D atomic-force microscopy image of the SiO_2 microstructure on Si (100) ($15 \times 15 \times 10^3$ nm; $1 \times 1 \times 10^3$ nm)

The SiO_2 surface after laser irradiation is shown in Fig. 2.

The block diagram of the device for triad attachment and excitation of bending resonant vibrations in the SiO_2/Si wafer-plate surface is represented in Fig. 3.

The measurements of IF temperature dependences $Q^{-1}(T)$ were performed in the kHz frequency range of f at small amplitudes of elastic deformation $\varepsilon \approx 10^{-6}$ before and after X-ray irradiation dose $D_\gamma \approx 10^2$ Gy; 10^3 Gy; $5 \cdot 10^3$ Gy and electron irradiation with dose $D_{e-} \approx 10^{14}$ cm^{-2}, 10^{15} cm^{-2}.

Atomic-force microscopy (AFM) and optical supervision of microstructure by means of the microscope "LOMO MVT" were used. Ultrasound (US) impulse-phase method using computerized "KERN-4" in Fig. 4,

Fig. 2 – SiO_2 surface after nanosecond laser irradiation by the ruby laser with the intensity $I \approx 400$ Mw/cm^2 with the dose $D = 5 \times I$ and the ruby laser pulse duration $\tau \approx 20$ ns with the wavelength $\lambda = 694$ nm ($\times 98$)
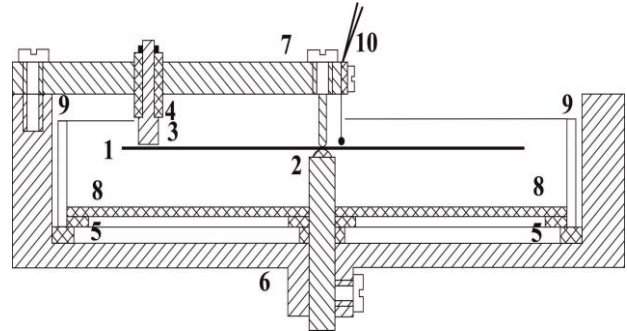

Fig. 3 – Block diagram of the device for triad attachment and excitation of bending resonant vibrations in the SiO_2/Si wafer-plate: 1 – disk-shaped SiO_2/Si wafer-plate, 2 – triad mounting of the SiO_2/Si wafer-plate, 3 – copper capacitive sensor for excitation and reception of bending resonant vibrations, 4, 5 – ceramics, 6 – copper holder body, 7 – steel half-cover of the holder body, 8 – tungsten furnace, 9 – heat shield, 10 – thermocouple

Fig. 5, with frequencies $f^\perp \approx 0.7$ MHz and $f_\parallel \approx 1$ MHz was used [16-19]. The measured velocity error was equal to $\Delta V/V \approx 1.5$ %.

All the molecular dynamics simulations were performed using the large-scale atomic/molecular massively parallel simulator software. We used the Tersoff empirical potential to account for the interactions among silicon atoms. This potential has been shown to be reliable for studying the structural and thermal properties of Si nanostructures [20]. The number of atoms in the model was 80000. The coordinate systems of the Si lattice arrangement were set to x [1 0 0], y [0 1 0], and z [0 0 1]. A time step of 1.0 fs with the Velocity-Verlet integration algorithm was used in all simulations. To eliminate the internal stress of the system, the structure was firstly energy-minimized using the conjugate gradients method and then equilibrated using isobaric (NPT) ensemble MD simulation for 500 ps at 300 K and a pressure of 0 atm.

After this, an NVT ensemble was used to deform the simulation box in desired directions with constant engineering strain-rate $d\varepsilon / dt = 10^8$ s^{-1}. During the loading process, the pressure in the other two directions was always set to zero except for the z-direction where the deformation was applied. Tensile stress of the system at each strain level in the direction of load is calculated when the diagonal components of the stress tensor per atom are summed for all atoms and the sum is divided by the volume of system, which is explained by the Virial equation:
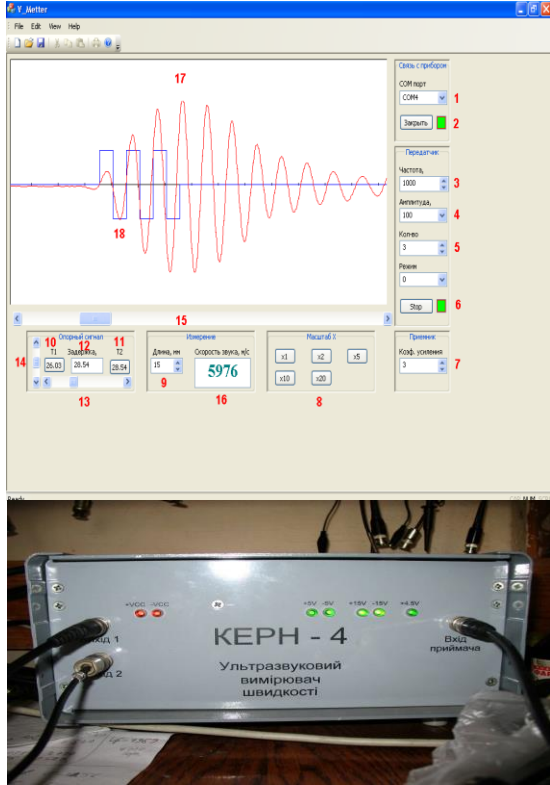
Fig. 4 – Illustration of the window for processing data of elastic waves velocity $V_\parallel$ measurements by echo-pulse method and the presence of computer device KERN-4
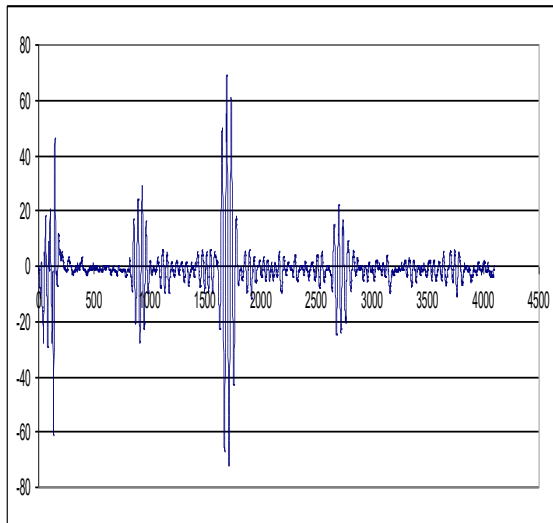

Fig. 5 – Oscillogram of transverse polarization impulses V_{S1} in the SiO₂/Si wafer-plate

$$\sigma_{ij} = \frac{1}{V}\left(\frac{1}{2}\sum_{\alpha=1}^{N}\sum_{\beta\neq\alpha}^{N} U\left(r^{\alpha\beta}\right)\frac{\Delta x_i^{\alpha\beta}\Delta x_j^{\alpha\beta}}{r^{\alpha\beta}} \right), \qquad (1)$$

where i and j denote the components of Cartesian coordinates, N is the total number of atoms, $r^{\alpha\beta}$ is the distance between two atoms α and β, $\Delta x^{\alpha\beta} = x^\alpha - x^\beta$, U is the potential energy, and V is the volume of the system.

The stress-strain curves contain fundamental information about the mechanical properties of the material during tensile deformation. Fig. 6 shows the stress-strain tensile curves of the silicon crystal at room temperature. At initial deformation stage, the stress and strain increase linearly which is expected from single-crystalline silicon behavior. After passing the linear deformation and with applying a larger strain value, the curve becomes slightly nonlinear, and the stress reaches its maximum of about 15 GPa. After the maximum, the stress has a sharp drop reflecting the brittle fracture of silicon.

We then performed the estimation of the elastic modulus E from the slope of the stress-strain $\sigma(\varepsilon)$ curve presented in Fig. 6, in the elastic deformation range ($\varepsilon < 2.0$ %). The elastic modulus of single-crystalline Si was 95 GPa. The results of calculating the elastic modulus using the linear part of the curves and experimental results show that there is a good agreement between these predicted results and experimental ones.
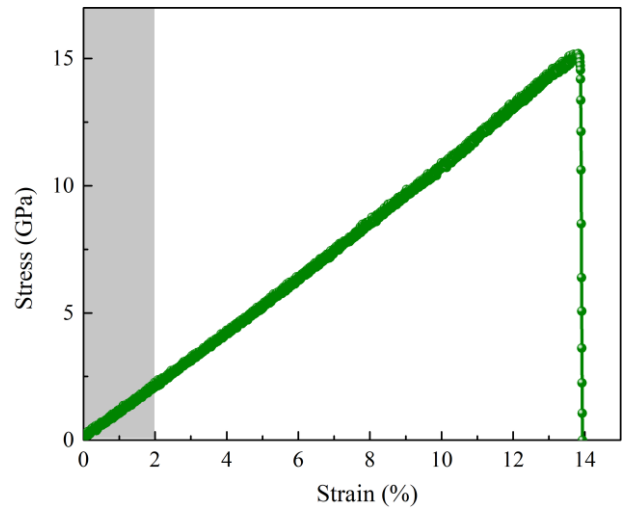

Fig. 6 – The room temperature stress-strain curve of single-crystalline Si obtained by molecular dynamics. The gray area corresponds to the elastic deformation stage to determine the elastic modulus

3. RESULTS AND DISCUSSION

The IF maximum at $T_{M1} \approx 330$ K increases sharply after X-ray irradiation with dose $D_\gamma \approx 10^2$ Gy; its height Q^{-1}_{M1} increases almost threefold with a twofold decrease in the width ΔQ^{-1}_{M1}, as shown in Fig. 7, which indicates the relaxation process of radiation defects of the same type.

Relaxation processes in SiO₂/Si are caused by processes occurring under the action of stress fields σ. The relaxation time τ of these processes is determined by their nature and is a material constant. The relaxation time of the processes associated with the migration of atoms is described by an exponential dependence [11]:

$$\tau = \tau_0 e^{\frac{H}{k_B T}}, \qquad (2)$$

where H is the activation energy of this relaxation process, τ_0 is the relaxation time constant, k_B is the Boltzmann constant, T is the temperature.

Equation (2) makes it possible to experimentally determine the activation energy H of the corresponding relaxation process from the temperature position of the
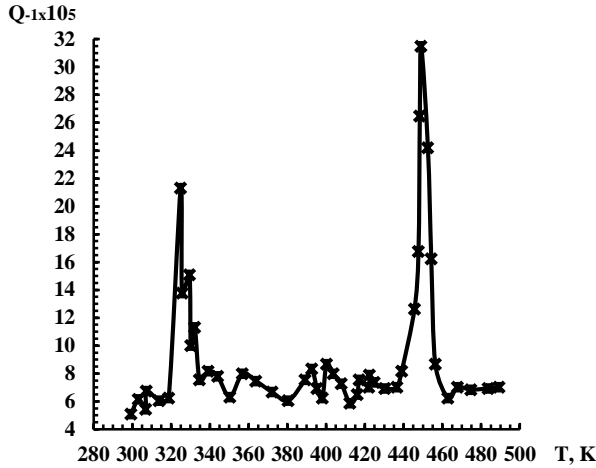
Q-1x105

Fig. 7 – Temperature dependence of the IF $Q^{-1}(T)$ in SiO₂/Si wafer-plate of *p*-type doped with *B*, KDB-7.5 (100); diameter $D \approx 76 \cdot 10^{-3}$ m, thickness $h \approx 460 \cdot 10^3$ nm with a SiO₂ layer thickness $h_{SiO_2} \approx 100$ nm after X-ray irradiation with dose $D_\gamma \approx 10^2$ Gy

IF peak $Q^{-1}(T)_M$. It is necessary to carry out measurements in the frequency range *f* with a change width Δf of at least one order of magnitude $\Delta f/f > 10$, which presents great experimental difficulties, to find the IF peak Q_M^{-1} under conditions of oscillation frequency change $\omega = 2\pi f$. IF Q^{-1} depends on product $\omega\tau$ [12]:

$$Q^{-1} = \frac{\Delta E}{E_R} \frac{\omega\tau}{1+\omega^2\tau^2}, \qquad (3)$$

where E_R is the relaxed or isothermal elastic modulus, E_N is the unrelaxed or adiabatic elastic modulus, $\Delta E = E_N - E_R$ is the elastic modulus defect. Therefore, the measurement of IF depending on ω $Q^{-1}(\omega)$ at constant τ can be replaced by the measurement of IF depending on τ $Q^{-1}(\tau)$ at constant frequency ω. It follows from equation (3), that IF value is the symmetric function of the product $\omega\tau$. There is a frequency range in which the mechanical energy loss Q^{-1} and the defect of the elastic modulus ΔE have maximum values between two extreme values of high ($\omega \to \infty$) and low ($\omega \to 0$) frequencies. The IF maximum value is $Q^{-1} = \frac{\Delta E}{2E_R}$, when $\omega\tau = 1$, but the variable may not be frequency ω, but the relaxation time τ.

For the same IF value $Q^{-1}(T)_1 = Q^{-1}(T)_2$, the equality $\omega_1\tau_1 = \omega_2\tau_2$ should be realized, where indices 1 and 2 refer to different IF curves. Therefore, taking into account equation (2), the equality takes the form

$$\omega_1 e^{\frac{H}{k_B T_1}} = \omega_2 e^{\frac{H}{k_B T_2}}, \qquad (4)$$

from where we obtain the formula for determining the value of the activation energy of IF maximum $Q^{-1}(T)_M$:

$$H = \frac{k_B \ln\left(\frac{\omega_2}{\omega_1}\right)}{T_1^{-1} - T_2^{-1}}. \qquad (5)$$

The modern methods of measuring IF $Q^{-1}(T)$ allow temperature measurements at several fixed harmonic frequencies ω_1, ω_2.

The activation energy value $H_1 \approx 0.63 \pm 0.1$ eV was obtained from equation (5) for the IF peak Q_M^{-1} in the

Si plate at $T_{M1} \approx 330$ K in Fig. 8. The proximity of the obtained activation energy H_1 at $T_{M1} \approx 330$ K to the migration energy $H_0 \approx 0.85 \pm 0.1$ eV for positively charged interstitial atoms Si$_i^+$ suggests a relaxation mechanism due to the reorientation of positively charged interstitial atoms Si$_i^+$.

After irradiation with the dose $D_\gamma \approx 5 \cdot 10^3$ Gy, the IF Q^{-1}_{M1} maximum height at $T_{M1} \approx 330$ K did not change significantly in comparison with the IF $Q^{-1}(T)$ spectrum before irradiation that indicates a special effect of the dose $D_\gamma \approx 5 \cdot 10^3$ Gy. The second IF maximum at $T_{M2} \approx 450$ K, due to the reorientation of neutral interstitial atoms of Si$_i^0$ complexes in the dumbbell configuration, also increased significantly after irradiation. The annealing of radiation defects changes the shape of the temperature spectrum of IF $Q^{-1}(T)$. An increase in the radiation dose D_γ also leads to a change in $Q^{-1}(T)$, which is illustrated in Fig. 8.
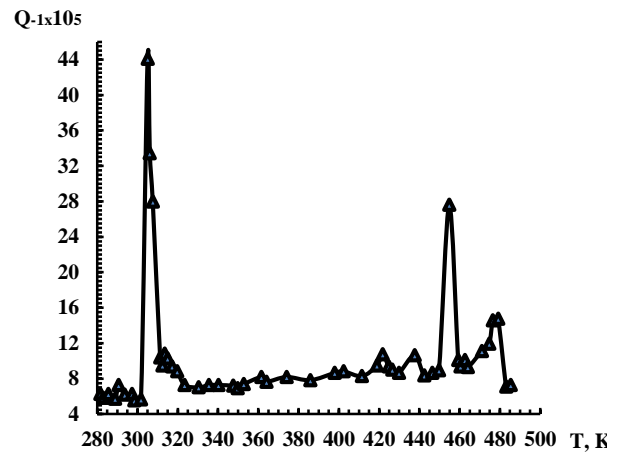
Q-1x105

Fig. 8 – Temperature dependence of the IF $Q^{-1}(T)$ in SiO₂/Si wafer-plate of *p*-type doped with B, KDB-7.5 (100); diameter $D \approx 76 \cdot 10^{-3}$ m, thickness $h \approx 460 \cdot 10^3$ nm with a SiO₂ layer thickness $h_{SiO_2} \approx 100$ nm after X-ray irradiation with dose $D_\gamma \approx 5 \cdot 10^3$ Gy when reheated

After electron irradiation in Fig. 9 as a result of the collision of electrons *e⁻* with Si atoms, Frenkel defects such as vacancy-interstitial atoms *V*-Si$_i$ are formed. Calculations show that the electron energy $W \approx 1$ MeV, which corresponds to the experiment, is sufficient to shift Si atoms from their equilibrium positions.

The area of the curve in Fig. 10 at the frequency $f = 200 \div 500$ kHz at attenuation $\alpha \approx 70$ dB is proportional to the power of the neodymium laser $I(S)$ and proportional to the acoustic oscillations $W(S)$ energy [18, 19].

The acoustic emission (AE) is the threshold phenomenon, so the certain threshold of the equipment operation is set. This is done in order to limit the intrinsic noise of devices and interference, which interfere the effective registration of the actual AE signals. It is important to correctly determine the possible AE mechanisms. The sequence in time is as follows: 1) AE at the melt of the quartz surface is the solid-liquid phase transition, 2) AE at the solidification of the melt is the liquid-solid phase transition, 3) AE at the crack formation. The processes at the solid-gas and gas-solid phase transitions due to relatively "long" nanosecond laser pulse

can be neglected. Under the conditions of the experiment, the phase transitions occur rather quickly – for a time that can be compared with the laser exposure time $\tau \approx 20$ ns, the formation of the "acousto-emission part" of the acoustic response is associated with the crack formation. The approach to AE as emission of two types: discrete (high-energy) and continuous (low-energy) is leveled for cases when the duration τ of individual AE acts exceed the time of the mineral wave $\tau > t$, and the linear wavelengths λ are linear rock dimensions λ, L.
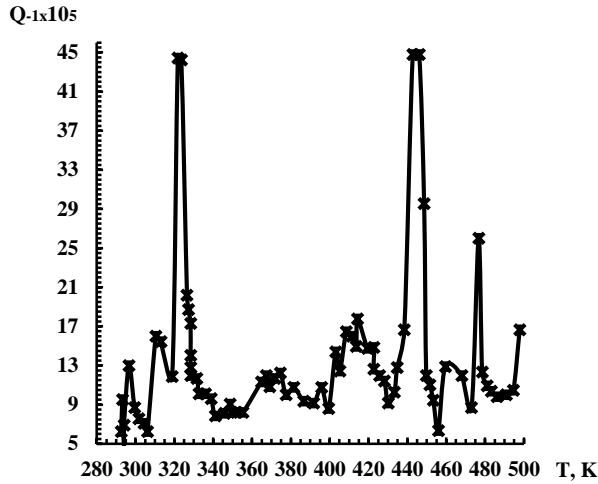

Fig. 9 – Temperature dependence of the IF $Q^{-1}(T)$ in SiO₂/Si wafer-plate of p-type doped with B, KDB-7.5 (100); diameter $D \approx 76 \cdot 10^{-3}$ m, thickness $h \approx 460 \cdot 10^3$ nm with a SiO₂ layer thickness $h_{SiO_2} \approx 100$ nm after electron irradiation with energy $W_{e-} \approx 1.5$ MeV and dose $D_{e-} \approx 10^{14}$ cm^{-2}

The depth of the broken layer h_b and the dislocation density n_d are determined from the IF difference ΔQ^{-1} on the nearby harmonics f_1 and f_2 after mechanical and heat treatments. The linear dependence of the IF difference ΔQ^{-1} of the SiO₂ + Si wafer-plate on the depth of the broken layer $h_b = 1000 \div 3000$ nm is demonstrated in Fig. 11.

The logarithmic decrement of US attenuation δ of oscillations with the amplitude $A = A_0 e^{-\delta x}$ is equal to:

$$\delta = ln\left(\frac{A_{n+1}}{A_n}\right). \tag{6}$$

The shear modulus $G = \rho V\perp^2$, the elastic dynamical modulus E [10]:

$$E = \rho V\perp^2 \left[3 + \frac{1}{1 - \left(\frac{V_\parallel}{V_\perp}\right)^2}\right], \tag{7}$$

where $V\perp$ is the quasitransversal US velocity.

The Poisson coefficient μ is equal to the ratio of the relative transversal $\varepsilon\perp$ compression to the relative longitudinal lengthening $\varepsilon_\parallel$ [11]:

$$\mu = -\frac{\varepsilon_\perp}{\varepsilon_\parallel} = -\frac{\frac{\Delta X}{X}}{\frac{\Delta l}{l}} = -\frac{\Delta X}{\Delta l} * \frac{l}{X}, \tag{8}$$

$$\mu = \frac{\frac{1}{2}V_\parallel^2 - V_S^2}{V_\parallel^2 - V_S^2}. \tag{9}$$
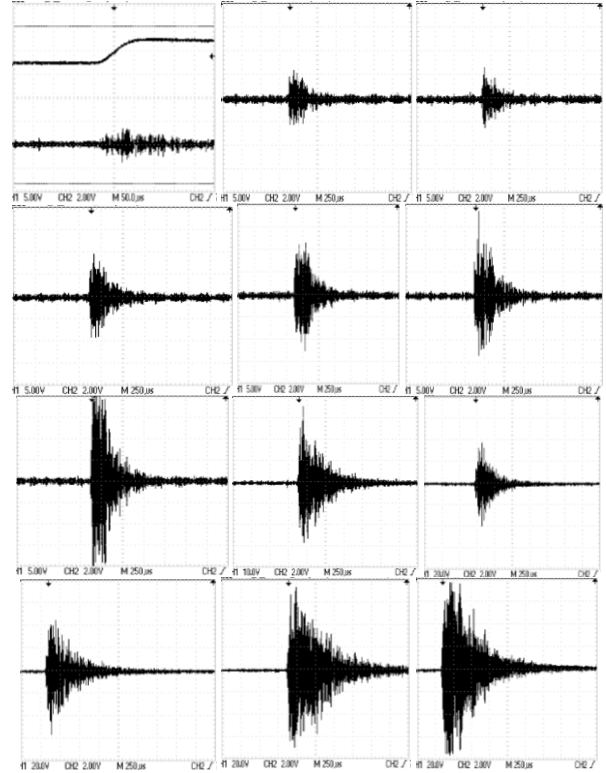

Fig. 10 – Acoustic emission signal after the neodymium laser irradiation with different intensity: $I = 10$, 40, 70, 100, 140, 180, 230, 250, 290, 340, 400, 450 MW/cm²
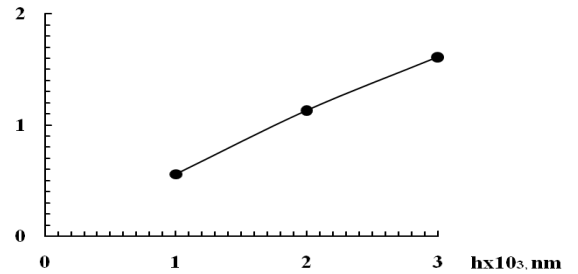

Fig. 11 – Dependence of the IF difference ΔQ^{-1} of the SiO₂ + Si wafer-plate on the depth of the broken layer h_b

One oscillator produces 3 waves: 1 longitudinal and 2 transverse. The Debye temperature θ_D was determined by the formula [12]:

$$\theta_D = \frac{h}{k_B} * \left(\frac{9N_A\rho}{4\pi A}\right)^{\frac{1}{3}} * \left(\frac{1}{V_\parallel^3} + \frac{2}{V_\perp^3}\right)^{\frac{1}{3}}, \tag{10}$$

where h is the Plank constant, N_A is the Avogadro number, A is the middle gram-molecular mass.

4. CONCLUSIONS

1. The results of evaluation of the dynamic characteristics of interstitial atoms Si$_j$, vacancies V and O-complexes after X-ray irradiation can be used to take into account the annealing conditions in order to obtain specific structural defects in the SiO₂/Si wafer.

2. The study of vibrations of a disk semiconductor at different harmonic frequencies f_0, f_2 made it possible to develop the technique for determining the structural defect density n_D for the SiO_2/Si wafer-plate.

3. Internal friction Q^{-1}, shear modulus G, elastic modulus E, Poisson coefficient μ depend on anisotropy of the SiO_2/Si wafer-plate.

4. The relationship between the internal friction difference ΔQ^{-1} and the depth of the broken layer h_b was established for SiO_2/Si wafer-plates.

5. The growth of the internal friction maximum height Q_M^{-1} testifies the growth of the structural defect concentration n, and the broadening of internal friction maximum ΔQ_M^{-1} here represents the relaxation process of structural defects of new types in SiO_2/Si wafer-plate.

ACKNOWLEDGEMENTS

REFERENCES

1. A.P. Shpak, Y.A. Kunickiy, V.L. Karbovskiy, *Cluster and Nanostructural Materials* (Kyiv: Academy Periodic: 2001).
2. V.B. Molodkin, A.I. Nizkova, A.P. Shpak, et al., *Difractometria Nanosize Defects and Geterolayers in Crystals* (Kyiv: Academy Periodic: 2005).
3. A.V. Udovenko, G.V. Markova, R.N. Rostovtsev, *Microstructure and Properties of Mn-Cu Alloys System* (Tula: TNTU: 2005).
4. M.S. Blanter I.S. Golovin, H. Neuhauser, H.-R. Sinning, *Internal Friction in Metallic Materials. A Handbook* (Springer Verlag, Berlin: Heidelberg: 2007).
5. V.T. Grinchenko, I.V. Vovk, V.T. Matsipura, *Basics of Acoustics* (Kyiv: Naukova dumka: 2007).
6. N.A. Azarenkov, V.M. Beresnev, A.D. Pogrebnyak, *Structure and Properties of Protective Covering and Modify Materials Layers* (Charkov: CNU: 2007).
7. A.I. Akishin, *Space Materials Science* (Moscow: Publishing company MSU: 2007).
8. V.V. Pogosov, Y.A. Kunickiy, A.V. Babich, A.V. Korotun, A.P. Shpak, *Nanophysics and Nanotechnologies* (Zaporizhia: ZNTU: 2011).
9. I.S. Golovin, *Internal Friction and Mechanical Spectroscopy of Metal Materials* (Moscow: Publishing company MISIS: 2012).
10. R. Schaller, D. Mari, *Internal Friction and Mechanical Spectroscopy* (Switzerland: Trans Tech Publication: 2012).
11. I.S. Golovin, *Anelasticity, Internal Friction and Mechanical Spectroscopy of Metallic Materials* (Moscow: Publishing company MISIS: 2020).
12. I.S. Golovin, S.V. Divinski, J. Čížek, I. Procházka, F. Stein, *Acta Mater.* **53**, 2581 (2005).
13. I.S. Golovin, *Mater. Des.* **88**, 577 (2015).
14. V. Babich, V. Dovbenko, L. Kuzmych, T. Dovbenko, *MATEC Web of Conferences* **116**, 02005 (2017).
15. I.S. Golovin, V.V. Palacheva, J. Cifre, C. Jiang, *J. Alloy. Compd.* **785**, 1257 (2019).
16. A.P. Onanko, V.V. Kuryliuk, Y.A. Onanko, A.M. Kuryliuk, D.V. Charnyi, M.P. Kulish, O.P. Dmytrenko, *J. Nano- Electron. Phys.* **12** No 4, 04026 (2020).
17. I. Korobiichuk, V. Drevetsky, L. Kuzmych, I. Kovela, *Automation 2020* **1140**, 87 (2020).
18. A.P. Onanko, D.V. Charnyi, Y.A. Onanko, M.P. Kulish, O.P. Dmytrenko, S.A. Popov, *Conference Proceedings of 18th International Conference on Geoinformatics – Theoretical and Applied Aspects* **2019**, 1 (2019).
19. A.P. Onanko, D.V. Charnyi, Y.A. Onanko, M.P. Kulish, O.P. Dmytrenko, R.V. Homenko, *Conference Proceedings of Geoinformatics: Theoretical and Applied Aspects 2020* **2020**, 1 (2020).
20. V.V. Kuryliuk, S.S. Semchuk, K.V. Dubyk, R.M. Chornyi, *Nanostructures and Nano-Objects* **29**, 100822 (2022).

Механічна спектроскопія і внутрішнє тертя в SiO₂/Si

А.П. Онанко[1], В.В. Курилюк[1], Ю.А. Онанко[2], А.М. Курилюк[1], Д.В. Чарний[2], О.П. Дмитренко[1], М.П. Куліш[1], Т.М. Пінчук-Ругаль[1], А.А. Кузьмич[3]

[1] *Київський національний університет імені Тараса Шевченка, вул. Володимирська 64/13, 01601 Київ, Україна*
[2] *Інститут водних проблем і меліорації, вул. Васильківська 37, 03022 Київ, Україна*
[3] *Національний університет водного господарства та природокористування, вул. Соборна 11, 33000 Рівне, Україна*

Розроблена методика, сконструйована та виготовлена установка для збудження та реєстрації затухаючих згинних резонансних коливань в SiO₂/Si дископодібних підкладках товщиною $h = 300 \div 500 \cdot 10^3$ нм та діаметром $D = 60 \div 100 \cdot 10^6$ нм з метою вимірювання структурно-чутливого внутрішнього тертя (ВТ) Q^{-1}. Розроблена методика неруйнуючого контролю інтегральної густини структурних дефектів n_∂ та глибини порушеного шару $h_{пш}$ у дископодібних напівпровідникових підкладках. Вимірювання фону ВТ Q^{-1}_0 на гармонійних частотах f_0, f_2 дозволило експериментально визначити вузлові лінії дисків, що коливаються. Це дозволило вносити поправки до теоретичних розрахунків знаходження цих вузлових ліній з урахуванням лінійних розмірів дисків та способу їх кріплення. Досліджено температурний спектр ВТ $Q^{-1}(T)$ в SiO₂/Si дископодібних підкладках після їх рентгенівського та електронного опромінення. В процесі вимірювань було встановлено, що відпал структурних дефектів Si змінює форму температурного спектру ВТ $Q^{-1}(T)$. Піки ВТ Q^{-1}_M, що утворюються точковими дефектами, можна було спостерігати при умові, коли підкладка Si нагрівалася зі швидкістю $V = \Delta T/\Delta t \leq 0.1$ К/с. Це дозволило

визначити енергію активації H переорієнтації анізотропних комплексів радіаційних дефектів. Встановлення стабільності параметрів фону ВТ Q^{-1}_0 дає можливість визначити радіаційну стійкість напівпровідникових підкладок та виробів на їх основі. Запропонована методика може використовуватись як неруйнуючий метод контролю дефектності кристалічної структури напівпровідникових підкладок, що застосовуються для потреб мікроелектроніки.

Ключові слова: Механічна спектроскопія, Релаксаційний механізм, Підкладка, Міграція атомів, Внутрішнє тертя.